VOL. 13, NO. 21, NOVEMBER 2018 ISSN 1819-6608
ARPN Journal of Engineering and Applied Sciences
©2006-2018 Asian Research Publishing Network (ARPN). All rights reserved.
www.arpnjournals.com

DESIGN MATHEMATICAL MODEL FOR HEAT TRANSFER IN LASER BEAM WELDING PROCESS

Rafel Hekmat Hameed and Isam Mejbel Abed
Department of Mechanical Engineering, College of Engineering, University of Babylon, Iraq
E-Mail: eng_rafal@yahoo.com

ABSTRACT

The model of energy transport is designed to include the fusion effects by using a moving boundary problem. This model allows accounting for both high order temperature gradients and state of non-equilibrium, this prompts further realistic determination the distribution of temperature within the work-piece. The model has been employed to simulate the evolution of spatial temperature distribution within the target materials when irradiated with both CW and pulsed laser. This model explains the welding process in terms of the velocity of fusion surface (V_*) which has been calculated as a function of power intensity. The zone of fusion dimensions, and the heat affected zone are illustrated of target metal with phase transformation under the incident power intensity in a range of 10^5 W/cm^2. A new scheme of welding mechanism has been implemented. This scheme is based on switching from the transient model of welding to continuous welding (steady state), using a lagging method in explicit technique. This method gives more stable solution through a computer program, which calculates the temperature distribution from a moving work-piece.

Keywords: fusion, laser beam, heat transfer, mathematical model, welding, moving boundary.

1. INTRODUCTION

Welding by a high-power CO_2 laser is most used in industry today. This process is classified as a moving case. Many chemical and physical parameters are interested in this case. It is very difficult to obtain results when considering all the parameters. Fusion welding is one main fabrication process. In welding applications the laser parameters must be tailored so that undesired vaporization of the surface does not occur while achieving the desired molten depth. There are numerous workable applications which laser welding attained to production status. It is compete with several technique. In these situations, the laser process proffers advantages that are substantial for the workable application. These include: The loss of physical contact with localized heating, the electrode and prompt cooling because of the small laser spot and high heat flux. The ability to weld numerous various minerals and various geometries, and the capability to weld components in a controlled atmosphere or sealed within optically transparent materials.

Bertolotti and Sibilia [1981] explained analytical solutions for the penetration of the melting front that was found by resolving the equation of fusion interface motion. Itgotten by the conduction heat equation for the liquid area, and by the energy conservation at the fusion front. Solutions are gained both for constant and Gaussian light beams and for the case of constant thermal properties, whilst introducing the thermal conductivity discontinuity at the fusion interface. Liu and Asibu [1998] anticipated moving adaptive finite element analysis for dual - beam laser welding tailored blanks. The phase change impact, temperature reliance to the properties of material, both radiation and convection heat transfer are regarded. Only four-node quadrilateral finite elements have utilized in this model. However, they assumed it is lumped in the orientation of z-axis, and resolves for temperature averaged over the thickness. Error happens from the simplifying the model of finite element, which consists the contact boundary condition, disregard the evaporation pulls and flow of in the weld pool.

Mahrle and Schmidt [1998] showed a model for the emulation of the temperature dispensation through deep penetration laser beam welding of a fine sheets. The temperature reliance of the material properties is counted. For a steady state, the impact of the convective heat transfer is taken based on a numerical resolution of the Navier-Stokes equations. The calculation is carried out employ a finite difference scheme on staggered grids. This simulation of the temperature distribution is limited to thin sheets while Piekarska *et al.*, [2014] developed a mathematical model in three dimensions of the welding process by using Yb:YAG laser beam. This model was simulated by using a finite volume method to predict the temperature distributions through the welding pool and heat affected zone (HAZ). The resource of laser heat is calculated by the method of kriging interpolation. Experimental work was done on S355steel metal. Azizpour *et al.*, [2015] predicted a model in a three-dimensional by using the finite element code (*SYSWeld*) to simulate of laser beam welding of Ti6A14V sheet. They demonstrated the temperature distribution and weld geometry. They used a continuous wave mode CO_2 laser with the maximum power of 2.2 kW. In addition, they investigated the effect of focal position, power, speed, and the shapes of molten pool. Mwema [2017] used the solid works software to predict the transient temperature profiles through the welding process of metallic and non-metallic materials using moveable laser power resource. Also, the welding bead shape and the thermal profile for Nd:YAG laser welding operation of AISI304 steel lap joint has been elaborated. The result explains that the temperature close to the resource of the laser very high contrasted with that close to the edge. In addition, this study indicated that the depth of the beam penetration rise with increasing the power intensity of a laser. The equation of moving without give any solution. It produced

©2006-2018 Asian Research Publishing Network (ARPN). All rights reserved.

an interpolation equation to give the relationship between the velocity movements with the power intensity supplied by the laser source. From above researchers, nobody took the effect of phase transformation in simulation software, and the moving of a work piece through welding process.

In the present, a model in a three-dimensional finite difference method with implicit technique is predicted to simulate the transient temperature distribution in fusion and heat affected zones due to the effective of phase transformation (solid-liquid interface) and fusion latent heat of metal by using continuous mode of CO_2 laser through the welding process. In addition, the new scheme in a steady state is presented in order to explain the moving of work-piece through the welding process.

2. THERMAL PHENOMENA

Continuous wave (CW) laser working at output power in a practical system in the 10-20 kW range is currently available with the wave length of 10.6 Mm. It used for welding where scale effects have allowed the accomplishment of welding configurations. The metal used S355 steeland heated with a CO_2 laser beam of 10^5 W/cm^2 irradiance and 0.2 mm spot diameter. The numerical solution of distributing source has been utilized to simulate the temperature distribution. In the current work, considered that total laser power is the incident over a roundabout region. The dispersions of intensity inside the focus is a complex function of position and time, however, laser-induced thermal effect do not appear to be excessively sensitive to this distribution as long as that the temperature is inspected far from the immediate zone this imply that the association happens. Consequently, usually advantageous to expect as over that all the five structure in the intensity distribution is lost and that all the five structure in the intensity distribution is lost and that the thermal effect is the equivalent as that which would be delivered by absorption of the equivalent total power over a round zone whose radius may be picked empirically. The laser radiation is absorbed within a definite depth of the material thickness. The temperature distribution is to be calculated within the layer at which the laser radiation is absorbed. The absorption of laser energy eventuates in a layer being 10^{-6}-10^{-5} cm thick. Since, for the applicable laser intensities the width of the warmed area is normally numerous microns, one can portray the ingestion layer by surface heat input. Therefore, material is assumed to change from solid to liquid without any extra energy being required. It has accepted that the thermal constants autonomous of both the laser force and the temperature. The reflectivity of a metal surface is an important parameter, which controls the fraction of the laser radiation absorbed.

The reflectivity is a function of temperature and wavelength of the metal. At 10.6 µm wavelength, the reflectivity of the surface for the cold metal is much higher. The laser-metal interaction mechanism is dependent mainly on the laser pulse power intensity, duration, wavelength, and on the target material thermo-physical properties that were detailed by Ready [1978].

3. MATHEMATICAL ANALYSIS

Heat equations have been used to describe conduction within the metal irradiated with fast and rise time, high intensity pulses. It is important to determine the temperature profile in metals accurately, since the temperature distribution within the work-piece greatly affects phase transitions and hence, machining characteristics. Therefore, new models must be sought to reduce this discrepancy. In order to facilitate reasonable analysis of the welding process, a number of assumptions and simplifications have to be made to solve the two models which are describing this process. There are:

a) The intensity of a laser beam in W/cm^2 is adequate to the reason fusing of the front surface of the metal, which is in the range 10^4-10^5 W/cm^2.

b) The liquid, which is created due to the fusing of metals, is limpid to the energy of the incident laser.

c) Losses of heat due to re-radiant are negligible.

d) Beam focusing effects due to lensing are assumed ignore.

e) Invariable physical and thermal properties of irradiated metal while it is solid and liquid.

f) Take the effect of latent heat fusion or the quantity of heat required to raise the temperature to melting point.

g) In a new model predicted a mechanism of welding. New scheme does switching from unsteady transient state to steady state through moving of work- piece. This is the assumption in the scheme and uses the laser heat source, which varies exponentially with spatial distribution.

h) The metal is opaque, i.e., the laser beam does not penetrate noticeably into the medium, with unchanging absorptivity.

i) Losses of heat to the outside can be approximated utilizing a single, and steady the coefficient of heat transfer for both the radiative and the convective losses are dispensable.

The equation of heat conduction for a solid slab under a penetrating laser source at a three-dimensional is given by Dowden [2001]

$$\rho\, c_p \frac{\partial T}{\partial t} = \frac{\partial}{\partial x}\left(k\frac{\partial T}{\partial x}\right) + \frac{\partial}{\partial y}\left(k\frac{\partial T}{\partial y}\right) + \frac{\partial}{\partial z}\left(k\frac{\partial T}{\partial z}\right) + Q(x, y, z, t) \qquad (1)$$

The three-dimensional developed model in Cartesian coordinate has been assumed to give a solution to the equation (1) as the laser power is incident over a

©2006-2018 Asian Research Publishing Network (ARPN). All rights reserved.

rounded zone (πw^2). Figure-1 shows the coordinate system for the semi-infinite medium.

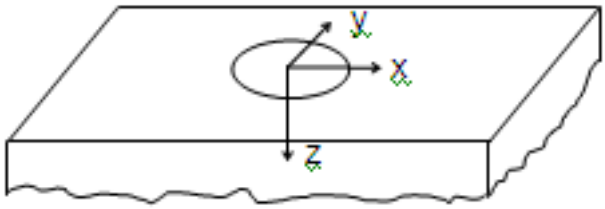

Figure-1. The system of cartesian coordinate.

Q is the resource term (heat production per unit volume per unit time) and it describes the absorption process as expressed by Bass [1983] as:

$$Q = (1-R)I\delta \, exp\left((-\delta z)\left(\frac{x^2+y^2}{w^2}\right)\right) \quad (2)$$

In the current work a new assumption has been made, that the absorption occurs in three directions. Then, the equation (2) becomes:

$$Q = (1-R)I\delta \exp\left(\left(-\delta\left(\sqrt{x^2+y^2+z^2}\right)\right)\left(\frac{x^2+y^2}{w^2}\right)\right) \quad (3)$$

Subject to the boundary conditions to illuminate equation (1) numerically:

$x \to \pm\infty$, $y \to \pm\infty$, $z \to +\infty$; $T \to T_\infty$; $z = 0$: $\frac{\partial T}{\partial z} = 0$

And the premier condition is $T(x, y, z, 0)=T_\infty$

A finite-difference method with implicit technique has been used to resolve the partial differential equation (1), so that the problem could be solved by a computer. It has been considered the approximation in the region over which we have laid an orthogonal grid with an equal spacing. Assuming Δx, Δy, and Δz equal 3 micrometer and Δt equal of 200 nanoseconds. The grid is represented by Figure-2.

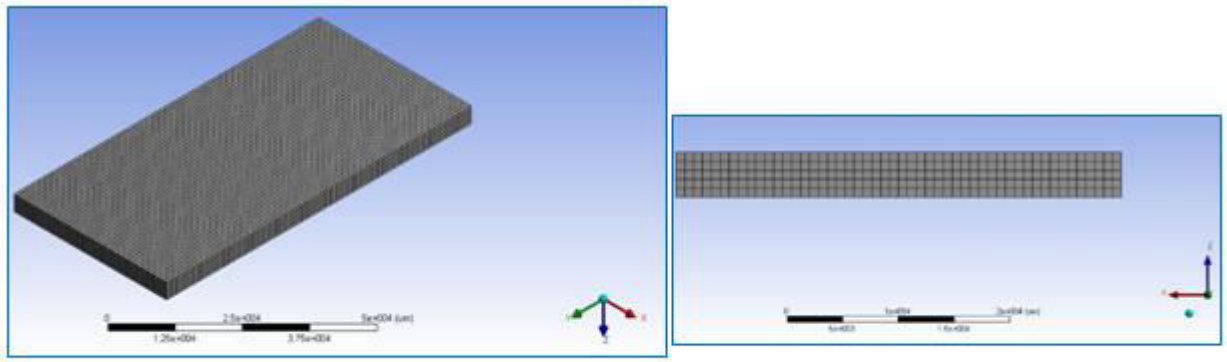

(a) 3D view of the model (b) Cross-section of the model

Figure-2. Geometry and mesh distribution.

The computer program gives more reliability to compute the temperature profile against x, y, and z coordinates depending upon the boundary conditions that gives a different form of the equation (1) in implicit finite difference technique. Principles of stability analysis with numerical schemes are illustrated by Petrovic and Stupar[1996]. The equation (1) can be written in finite difference form with implicit technique as:

$$T_{i,j,k}^{n+1} = \lambda T_{i+1,j,k}^{n+1} - 6\lambda T_{i,j,k}^{n+1} + \lambda T_{i-1,j,k}^{n+1} + \lambda T_{i,j+1,k}^{n+1} + \lambda T_{i,j-1,k}^{n+1} + \lambda T_{i,j,k+1}^{n+1} + \lambda T_{i,j,k-1}^{n+1} + \frac{Q}{k}\alpha\Delta t + T_{i,j,k}^{n} \quad (4)$$

a) At front surface in point (c) where x=y=z, and z=0 ,$\frac{\partial T}{\partial z} = 0$ as shown in Figure-3(a).

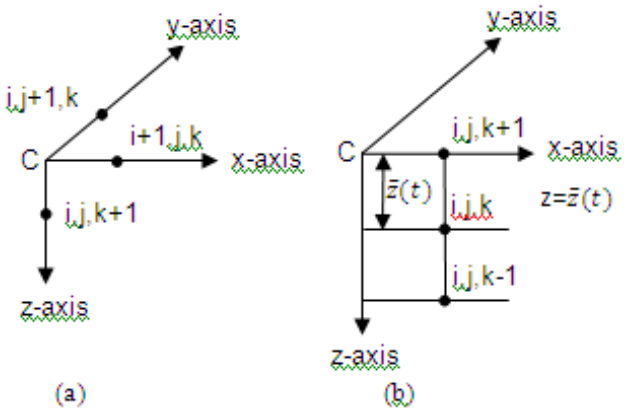

Figure-3. Types of fixed boundary condition.

The surface heating for short time until the surface temperature reaches melting point 1800 K, then equation (4) becomes

©2006-2018 Asian Research Publishing Network (ARPN). All rights reserved.

$$T_{i,j,k}^{n+1} = 4\lambda T_{i+1,j,k}^{n+1} + 2\lambda T_{i,j,k+1}^{n+1} - 6\lambda T_{i,j,k}^{n+1} + T_{i,j,k}^{n} + \frac{Q}{k}\alpha\Delta t \quad (5)$$

Where λ is the convergent $=\frac{\alpha\Delta t}{\partial x^2}$. Also, heating through x-axis, and y-axis where x→∞ and z=0 when $\frac{\partial T}{\partial z} = 0$. Then, equation (4) at x-axis becomes:

$$T_{i,j,k}^{n+1} = \lambda T_{i+1,j,k}^{n+1} - 6\lambda T_{i,j,k}^{n+1} + \lambda T_{i-1,j,k}^{n+1} + 2\lambda T_{i,j+1,k}^{n+1} + 2\lambda T_{i,j,k-1}^{n+1} + T_{i,j,k}^{n} + \frac{Q}{k}\alpha\Delta t \quad (6)$$

At y-axis

$$T_{i,j,k}^{n+1} = 2\lambda T_{i+1,j,k}^{n+1} - 6\lambda T_{i,j,k}^{n+1} + \lambda T_{i,j+1,k}^{n+1} + \lambda T_{i,j-1,k}^{n+1} + 2\lambda T_{i,j,k+1}^{n+1} + T_{i,j,k}^{n} + \frac{Q}{k}\alpha\Delta t \quad (7)$$

b)At z=$\bar{Z}$(t), when the fusing happen in this layer at x and y=0. Then, the boundary condition of phase transformation to liquidis referring to Figure-3-b. As energy balance at the surface necessitates that the energy given to the fusion material equivalents the energy conducted from the solid, hence

$$\rho L_m \frac{\partial \bar{z}(t)}{\partial t} = k_s \frac{\partial T}{\partial z}|_z = \bar{Z}(t) \quad (8)$$

$$\rho L_m V_* = k_s \frac{\partial T}{\partial z}|_z = \bar{Z}(t)$$
$$k_s \frac{T_{i,j,k+1} - T_{i,j,k-1}}{2\Delta z} = \rho L_m V_*$$
$$\therefore T_{i,j,k-1} = T_{i,j,k+1} - \frac{\rho L_m V_* 2\Delta z}{k_s} \quad (9)$$

Where $L_m$is the specific latent heat of fusion, and $V_*$is velocity of fusion surface and$\bar{Z}(t)$, z are the distance. Then, inserting the boundary condition of equation (9) in equation (1) becomes:

$$T_{i,j,k}^{n+1} = 4\lambda T_{i+1,j,k}^{n+1} - 6\lambda T_{i,j,k}^{n+1} + 2\lambda T_{i,j,k+1}^{n+1} - \lambda\frac{\rho L V_* 2\Delta z}{k_s} + T_{i,j,k}^{n} + \frac{Q}{k}\alpha\Delta t \quad (10)$$

Phase transformation also happens at z =$\bar{Z}(t)$, and x →∞. Then equation (4) becomes:

$$T_{i,j,k}^{n+1} = \lambda T_{i+1,j,k}^{n+1} - 6\lambda T_{i,j,k}^{n+1} + \lambda T_{i-1,j,k}^{n+1} + 2\lambda T_{i,j+1,k}^{n+1} + 2\lambda T_{i,j,k+1}^{n+1} - \lambda\frac{\rho L V_* 2\Delta z}{k_s} + T_{i,j,k}^{n} + \frac{Q}{k}\alpha\Delta t \quad (11)$$

Another Phase transformation through line y-axis at z =$\bar{Z}(t)$, and y→∞. Equation (4) Forms as:

$$T_{i,j,k}^{n+1} = 2\lambda T_{i+1,j,k}^{n+1} - 6\lambda T_{i,j,k}^{n+1} + \lambda T_{i,j+1,k}^{n+1} + \lambda T_{i,j-1,k}^{n+1} + 2\lambda T_{i,j,k+1}^{n+1} + T_{i,j,k}^{n} - \lambda\frac{\rho L V_* 2\Delta z}{k_s} + \frac{Q}{k}\alpha\Delta t \quad (12)$$

Steen and Kamalu [1983] show from a simple one-dimensional heat balance that the velocity of the fusion front into work-piece is given by the expression:

$$V_* = \frac{(1-R)I}{(\rho L_m + \rho c(T_L - T_m))} \quad (13)$$

c)Liquid phase: When z>$\bar{z}(t)$, and z →∞ , the fusion of metal starting and moving in fusion zone with velocity of fusion V_*, then equation (4) is formed as conduction energy equation as:

$$\frac{1}{\alpha}\frac{\partial T}{\partial t} + \frac{V_*}{\alpha}\frac{\partial T}{\partial z} = \frac{\partial^2 T}{\partial x^2} + \frac{\partial^2 T}{\partial y^2} + \frac{\partial^2 T}{\partial z^2} + \frac{Q}{k} \quad (14)$$

This equation is applied through z-axis, x-z, and y-z planes. After z >$\bar{z}(t)$, equation (14) becomes as:

$$T_{i,j,k}^{n+1} = 4\lambda T_{i+1,j,k}^{n+1} - 6\lambda T_{i,j,k}^{n+1} + (\lambda - \frac{V_*\Delta t}{2\Delta z})T_{i,j,k+1}^{n+1} + (\lambda + \frac{V_*\Delta t}{2\Delta z})\lambda T_{i,j,k-1}^{n+1} + T_{i,j,k}^{n} + \frac{Q}{k}\alpha\Delta t \quad (15)$$

And through x-z plane is:

$$T_{i,j,k}^{n+1} = \lambda T_{i+1,j,k}^{n+1} - 6\lambda T_{i,j,k}^{n+1} + \lambda T_{i-1,j,k}^{n+1} + 2\lambda T_{i,j+1,k}^{n+1} + \left(\lambda - \frac{V_*\Delta t}{2\Delta z}\right)T_{i,j,k+1}^{n+1} + \left(\lambda + \frac{V_*\Delta t}{2\Delta z}\right)\lambda T_{i,j,k-1}^{n+1} + T_{i,j,k}^{n} + \frac{Q}{k}\alpha\Delta t \quad (16)$$

At y-z plane equation (14) becomes

$$T_{i,j,k}^{n+1} = 2\lambda T_{i+1,j,k}^{n+1} - 6\lambda T_{i,j,k}^{n+1} + \lambda T_{i,j+1,k}^{n+1} + \lambda T_{i,j-1,k}^{n+1} + \left(\lambda - \frac{V_*\Delta t}{2\Delta z}\right)T_{i,j,k+1}^{n+1} + (\lambda + \frac{V_*\Delta t}{2\Delta z})\lambda T_{i,j,k-1}^{n+1} + T_{i,j,k}^{n} + \frac{Q}{k}\alpha\Delta t \quad (17)$$

d)Upon the assumption number 7, the process planning scheme for current model of laser welding is composed of two steps:

a) The welding happens instantaneously after the fusion process which the temperature distribution at weld process is calculated by transient model which is reported in previous steps.

b) In welding process the differential equation governing heat flow within the work-piece will be:

$$\frac{u}{\alpha}\frac{\partial T}{\partial y} = \frac{\partial^2 T}{\partial x^2} + \frac{\partial^2 T}{\partial y^2} + \frac{\partial^2 T}{\partial z^2} + \frac{Q}{k} \quad (18)$$

Where u is the velocity of movement of work-piece relative to heat spot, where y is the flow of heat direction.

A new assumption in new scheme, it is the switching from transient model to simulate the welding process in one point to steady state scheme to move the fusion zone to the another points in the destination of y-coordinate.

The boundary conditions depend in on the value of temperature reached in adjacent fusion zone, which reached at least the melting temperature or more. The flow heat conduction equation (18) is nonlinear. This equation usually contains the coefficient that represents a function of the unknown function to be solved. Anderson

©2006-2018 Asian Research Publishing Network (ARPN). All rights reserved.

et al. [1984] showed that the lagging method is the technique to linearization procedure of equation (18), this method is approximated by the partial derivative$\frac{\partial T}{\partial y}$, which will be approximated by the forward-difference method along the y-direction $u^n \frac{T_{i,j,k}^{n+1} - T_{i,j,k}^{n}}{\Delta y}$. Then, equation (8) is represented with this method and becomes:

$$T_{i,j,k}^{n+1} = \frac{1}{u^n}(\lambda T_{i+1,j,k}^{n} + \lambda T_{i-1,j,k}^{n} + \lambda T_{i,j+1,k}^{n} + \lambda T_{i,j-1,k}^{n} + \lambda T_{i,j,k+1}^{n} + \lambda T_{i,j,k-1}^{n}) + (1 - \frac{6\lambda}{u^n}) T_{i,j,k}^{n} + \frac{Q_{i,j,k}}{k} \frac{\alpha \Delta x}{u^n} \quad (19)$$

Where $\lambda = \frac{\alpha}{\Delta x}$ at Δx=Δy=Δz, and u is consider to be known. The only unknown value in previous expression is the function $T_{i,j,k}^{n+1}$, which is calculated upon the value of function from the previous iteration$T_{i,j,k}^{n}$.

4. RESULTS AND DISCUSSIONS

The algorithm's emulation program of the CO_2 laser process of welding is used for a metal sheet made of S_{355} steel. It was heated with laser beam of 10^5 W/cm^2 irradiance and 0.2 mm spot diameter. The dimensions of sheet metal are (80×40×5) mm of length, width, and thickness respectively. This metal has been selected because it has less reflectivity at 10.6 µm also; it has lower thermal conductivity and thermal diffusivity than other metals. The space is discretised by computational grid with Δx = Δy = Δz = 3µm, and time interval is 200 nanoseconds. The thermal and optical properties are depicted in Table-1.

Table-1. Thermal and optical properties which are utilized in the simulation.

Properties	Symbol	Value
Solid Phasedensity	ρ_S	7800 kg.m^{-3}
Liquid Phase density	ρ_L	6800 kg.m^{-3}
Specific heat of solid phase	c_S	650 J.(kg.K)$^{-1}$
Specific heat of liquid phase	c_L	840 J.(kg.K)$^{-1}$
Solid phasethermal conductivity	k_S	45 W.(m.K)$^{-1}$
Liquid phase thermal conductivity	k_L	35 W.(m.K)$^{-1}$
Melting point	T_m	1800 K
Boiling point	T_b	3010 K
Latent heat of fusion	L_f	270 × 10^3 J.kg^{-1}
Thermal diffusivity	A	8.875× 10^{-6} m^2.s^{-1}
Absorption coefficient	Δ	5.6× 10^{-7} m^{-1}
Reflectivity	R [at 10.6 µm]	0.90
Absorptivity	A=(1-R) [at 10.6 µm]	0.1

Algorithm results give the description of spatial and temporal temperature distribution using 3-dimension Cartesian model at time intervals of 200 nanoseconds. These results seem to be more realistic to explain the spatial temperatures distribution against x, y, and z-axis. It should be mentioned that the temperature distribution in y-axis is the same as that distribution in x-axis.

Figure-4 shows the spatial temperature distributions at different time intervals at power intensity value of 10^5W/cm^2 through x-axis. Generally, the spatial temperature gradient near the surface is very steep returning to a shallow negative gradient as the target metal ambient temperature is approached. This effect is amplified as time evolves. These results designate a higher thermal profile near the surface. Once the welding process becomes significant. A large negative gradient is generated in the surface; this is consistent with the laws of thermodynamics as energy can only flow from a high to low temperature. That was pointed at high level intervals time at 2600 and 3400 nanoseconds. The maximum fusion zone happens at the surface is 3 µm. that means the phase transformation from solid to liquid was significant starting at time 2600 ns in x=0 and continuous until time 3400 ns at x=3 µm.

©2006-2018 Asian Research Publishing Network (ARPN). All rights reserved.

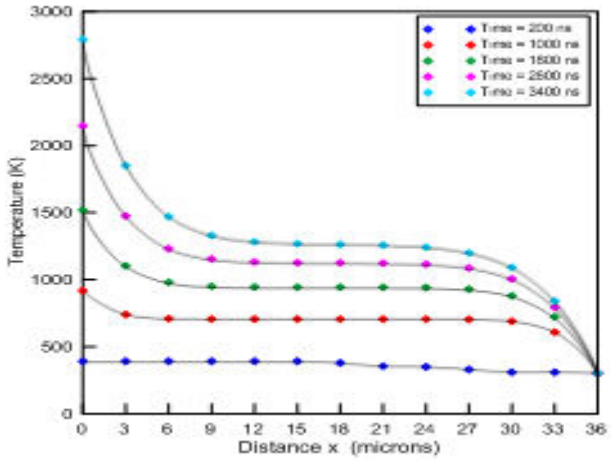

Figure-4. Temperature profile versus x-distance for various heating times in S_{355} steel at 10^5 W/cm^2.

Figure-5 illustrates the spatial temperature distribution at a different time intervals at I=10^5 W/cm^2 (in z-axis). A simulation of evolution of temperature profile was evaluated at the assumption of heat source was distributed. As the depth extents the laser radiation being absorbed at the layers next to the surface. This implies a less thermal gradient between these layers and the surface layer. Therefore, higher temperature levels can more likely, be maintained at the surface. It has been shown that the new model in the welding process gives a large positive gradient of temperature at the depth of metal because of the high energy melting material being removed. However, this phenomenon which is clearer in steel than other metals due to the properties and the lack of resolution of the z-axis.

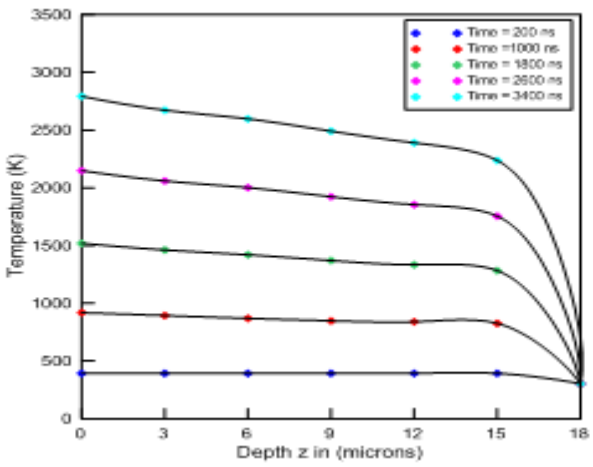

Figure-5. Temperature profile versus metal deep for various heating times in S_{355} steel at 10^5 W/cm^2

Figure-6 dominates the temporal distribution of temperature through the welding process. It was pointed that the temperature increases with increasing time. It has been indicated the time when the phase transformation from solid to liquid is started at time 2400 ns. That, it should be controlled the time of welding process and the value of the power intensity was used. That means to avoid reaching the boiling temperature (i.e. vaporization process). In the present analysis the model simulated the maximum time of welding process was 3400 ns and the temperature of fusion metal was reached to 2792.44 K.

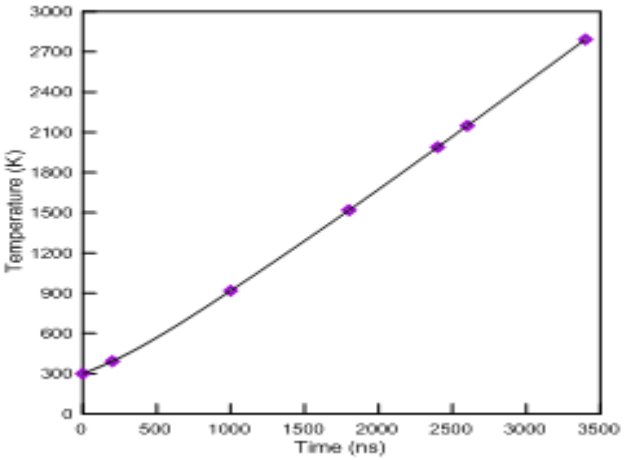

Figure-6. Temporal variation of temperature in S_{355} steel at 10^5 W/cm^2.

Figures-7 and 8 present the results in isothermal contours maps, which show the distribution of maximum temperature of melting pool on x-z surface at y=0 (from the face of the weld at the front surface) as illustrated in Figure-7.

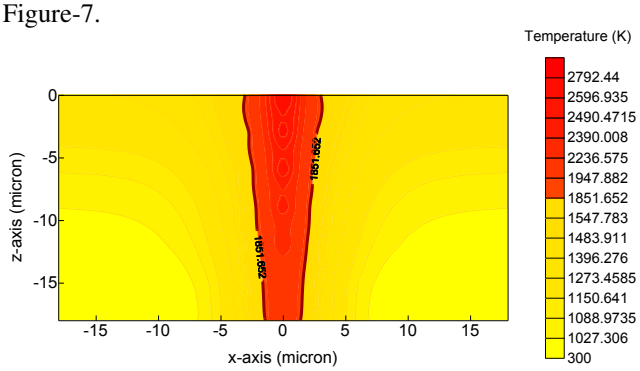

Figure-7. Isothermal contour of melting pool at front surface x-z, y=0 and time 3400 ns.

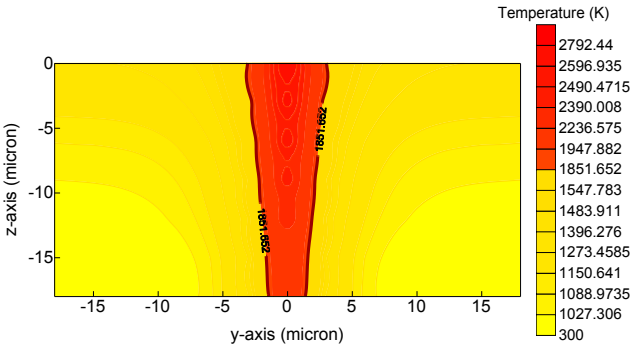

Figure-8. Isothermal contour of melting pool at side surface y-z, x=0 and time 3400 ns.

Figure-8 represents the isothermal contour in y-z plane at x=0 (from the face of the weld at the side

©2006-2018 Asian Research Publishing Network (ARPN). All rights reserved.

surface). These figures illustrate the fusion geometry diameter. Thus it can be seen that the fusion zone of diameter will depend upon laser power intensity, and metal thermal diffusivity varies with welding phase transformation velocity (i.e. V_* is the velocity of phase change from solid to liquid). This velocity was calculated as a function of power intensity. It is found from the prediction model the dimensions of melting pool. These are 3 microns in x and y axis as melt width at the front surface, and 15 microns as melt depth in z-axis. These results of temperature distributions of melting pool and its geometry are similar with experimental results, which were reported by piekarska*et al.*, [2014] even they used another type of laser.

Figures 9 and 10 show numerically calculated temperature distributions in the laser welding process. These figures explain the results of isothermal contours map for heat affected zone (HAZ) after fusion boundary on x-z plane, and y-z plane. It has been shown the temperatures values decrease after fusion boundary. These values are less than the melting point of metal (i.e. less than 1800 K). These figures are indicated the heat affected zone through the welding process. It is noted these values of (HAS) are 18 microns from the center of melting pool in x-axis, and 15 microns in z-axis. The temperature values reduce after melting line from 1752.502 K at 3 microns in the back surface of metal to 982.114 K at 18 microns through x-axis.

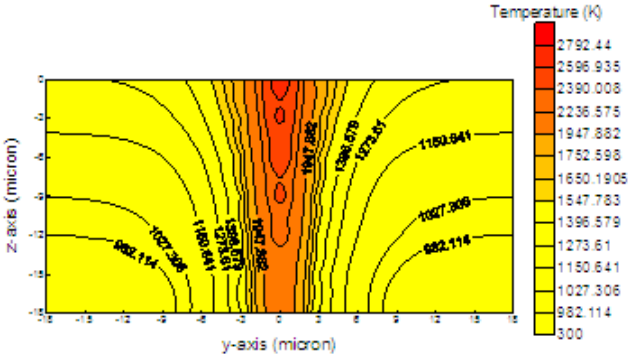

Figure-9. Isothermal contour of HAS at front surface (x-z),y=0, and time = 3400 ns.

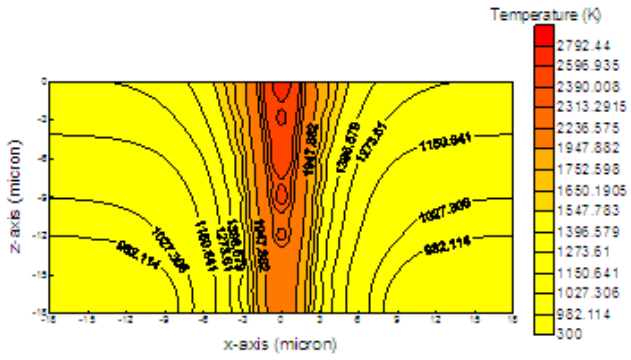

Figure-10. Isothermal contour of HAS at side surface (y-z),y=0,and time = 3400 ns.

Figures-11 and 12 dominate the heat penetration depth in metal more clearly through the welding process by estimating from numerical simulation in the face of the weld at the front surface x-z plane, and in the face at side surface of y-z plane. It was found the heat penetration depth reading until 38 microns in x and y axis, and 18 microns in depth z-axis.

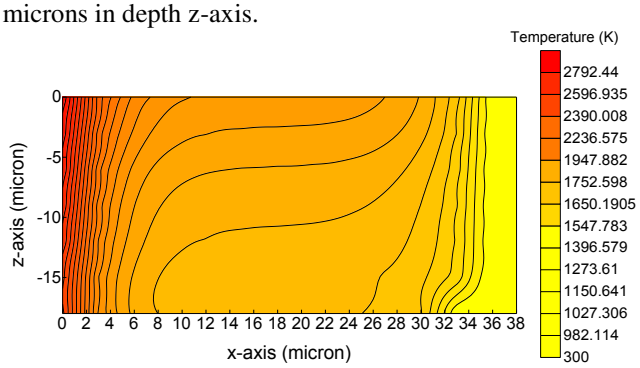

Figure-11. Isothermal contour of heat penetration depth at front surface x-z, y=0, and time 3400 ns.

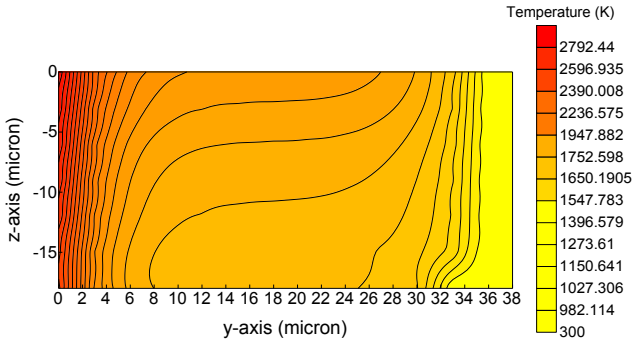

Figure-12. Isothermal contour of heat penetration depth at front surface y-z, x=0, and time 3400 ns.

Figure-13 demonstrates the three dimensional surface contour of temperature distribution through the entire domain of the welding process includes the melting pool, and heat affected zone. This surface contour represents the welding process dimensions in x-z plane with temperature distributions with time of 3400 nanoseconds. The melting pool zone is pointed at the centre of x-z plane in depth, and with 3 microns in width from the centre. Then, after the boundary of melting zone the heat affected zone is observed.

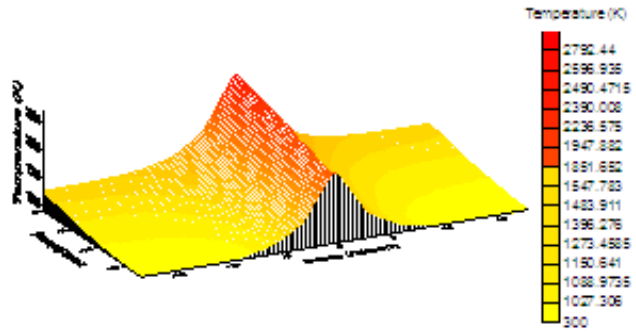

Figure-13. Surface contour of temperature distribution in three dimensions at time 3400 ns.

©2006-2018 Asian Research Publishing Network (ARPN). All rights reserved.

From the new scheme of equation (18) which was predicted the moving of the welding zone from point in section side of metal to another points in y-axis direction due to the moving of work-piece by different traverse speed. In that case, fusion pool must be moving in order to produce series points of welding through moving the work-piece in y-axis. Figures-14 and 15 dominate this phenomenon to show a series of the welding process produced with CO_2 laser at power intensity 10^5 W/cm^2 for S_{355} steel metal. These figures are produced at two values of traverse speed of work-piece under constant focusing conditions. It is seen that welding happened at the first time through the distance along three axes starting from zero distance of these axes until few microns. The solid line represents this process, which was simulated by a transient model at not moving the work-piece (i.e. u=0). Then, the fusion geometry of the welding process moves to another points in y-axis with two values of traverse speed as shown in these figures. The red dash line shows the switching from the transient model at stationary face to the new scheme in a steady state which was solved by lagging method. It is also seen that the temperature distribution of this metal decreases as the traverse speed is increased. Also, the temperature distribution was effected by the time of welding. It is indicated that temperature distribution increases with increasing the time of metal welding.

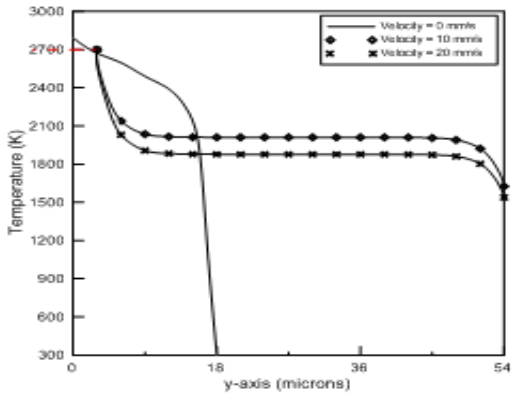

Figure-14. Temperature profile against y-distance for different travers velocities at I=10^5 W/cm^2,and time3400 ns.

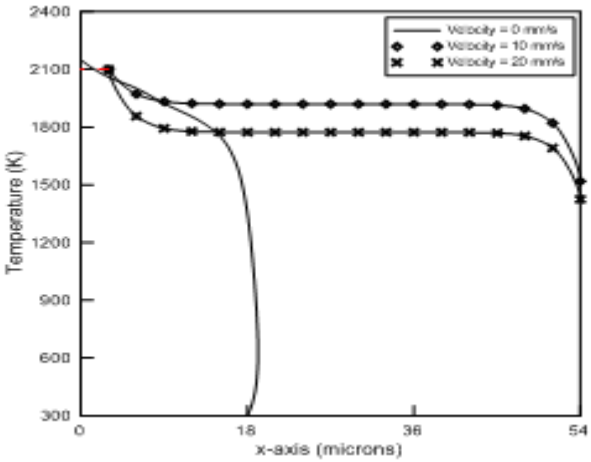

Figure-15. Temperature profile against y-distance for different travers velocities at I=10^5 W/cm^2, and time 2600 ns.

5. CONCLUSIONS

a) Theoretical investigation of the energy transport in metal caused by absorption of laser pulse radiation has been extended to include the effects of the fusion of the target metal with phase transformation (solid to liquid) under incident power intensity. This transient model demonstrates the welding process in terms of fusion velocity and the effect of fusion latent heat for the metal target. The algorithm simulation was solved by the implicit technique in finite difference method.

b) The spatial and temporal temperature distributions of fusion pool and heat affected zone are predicted by transient model. Their dimensions are illustrated by an isothermal contour map of the welding process at the front surface of metal in stationary point.

c) A new scheme is predicted to explain the continuous welding through the length of surface metal. It is the switching from transient model which simulating the welding process in one point at the front surface of target to steady state scheme for moving the fusion zone to another points in the direction of y-coordinate with two values of traverse speeds of work-piece.

d) Anew assumption of laser energy absorption in three dimensions (in x,y,and z directions) has presented in this work lead to more realistic results.

e) Laser wavelength effects have been considered implicitly within the reflectivity calculation and within the distributed heat source analysis. This means that the implemented simulation has taken all types of lasers into consideration.

©2006-2018 Asian Research Publishing Network (ARPN). All rights reserved.

REFERENCES

[1] Bertolotti M. and Sibilia C. 1981. Depth and Velocity of the Laser-Melted Front from an Analytical Solution of the Heat Conduction Equation. IEEE, Journal of Quantum Electronics. 17(10): 1980-1988.

[2] Liu Y. N. and Asibu E. K.1988. Finite Element Analysis of Heat Flow in Dual-Beam Laser Welded Tailored Blanks. J. Manufacturing Science and Engineering. 120: 272-278.

[3] Mahrle A. and Schmidt J.1998. Numerical Simulation of Heat Transfer during Deep Penetration Laser Beam Welding. Advanced Computational Methods in Heat Transfer, Editors: Nowak, A.J., Brebbia, C. A., Bialecki, R. and Zerroukat, M. Computational Mechanics Publications. UK.

[4] Piekarska W., Kubiak M., Saternus Z., Domanski T., Stano S., Radcenko M. V. and Ivanov S. G. 2014. Numerical Modeling of Thermal Phenomena in Yb:YAG Laser Welding Process. Journal of Applied Mathematics and Computational Mechanics. 13(3): 175-186.

[5] Azizpour M., Ghoreishi M. and Khorram A. 2015. Numerical Simulation of Laser Beam Welding of Ti6A14V Sheet. Journal of Computational and Applied Research in Mechanical Engineering. 4(2): 145-154.

[6] Mwema F.M. 2017.Transient Thermal Modeling in Laser Welding of Metallic / Nonmetallic Joints Using Solid Works Software. International Journal of Nonferrous Metallurgy. 6: 1-16.

[7] Ready J. F. 1978. Industrial Applications of Lasers. Book: Academic press. London.

[8] Dowden J.M. 2001. The Mathematics of Thermal Modeling-An Introduction to the Theory of Laser Material Processing. Book:Chapman$ Hall/ CRC. London.

[9] Bass M. 1983. Laser Material Processing. Book:North-Holland publishing company.

[10] Petrovic Z. and Stupar S.1996. Computational Fluid Dynamics. Book: Belgrade University press. Mechanical Eng. Faculty.

[11] Steen W.M. and Kamalu J.N. 1983. Laser Cutting. Laser Materials Processing Bass, M. Book: North Holland Publishing Company.

[12] Anderson D. A., Tannehill J., C. and Pletcher R.H. 1984. Computational Fluid Mechanics and Heat Transfer. Book: McGraw-Hill Publisher Company.